Photoanode Optimization on Dye-Sensitized Solar Cell Structure using Random Forest Method

Saputra, Marcus
Departmentiof Physics, Faculty of Mathematics and Natural Sciences, Sebelas Maret University

Supriyanto, Agus
Departmentiof Physics, Faculty of Mathematics and Natural Sciences, Sebelas Maret University

Purwanto, Agus
Department of Chemical Engineering, Faculty of Engineering, Sebelas Maret University

Paramitha, Tika
Department of Chemical Engineering, Faculty of Engineering, Sebelas Maret University

他

https://doi.org/10.5109/7236881

Photoanode Optimization on Dye-Sensitized Solar Cell Structure using Random Forest Method

Marcus Saputra[1,3], Agus Supriyanto[1,3,*], Agus Purwanto[2,3], Tika Paramitha[2,3],
Harry Kusuma Aliwarga[4], Shofirul Sholikhatun Nisa[3], Rifdha Hendianti Kisdina[3],
Rista Tristanti Kisdina[3], Nanda Yudi Shofi Subekti[3]

[1]Department of Physics, Faculty of Mathematics and Natural Sciences, Sebelas Maret University,
Jl. Ir. Sutami 36A, Surakarta 57126, Indonesia

[2]Department of Chemical Engineering, Faculty of Engineering, Sebelas Maret University,
Jl. Ir. Sutami 36A, Surakarta 57126, Indonesia

[3]Solar Cell Division, Centre of Excellence for Electrical Energy Storage Technology, Sebelas Maret University,
Jl. Slamet Riyadi no. 435, Laweyan, Surakarta 57146, Indonesia

[4]PT UMG Idealab, Jl. Tangkas Baru no. 2, Setiabudi, Jakarta Selatan 12930, Indonesia

*Author to whom correspondence should be addressed:
E-mail: agusf22@staff.uns.ac.id

Abstract: Dye-sensitized solar cell (DSSC) is significantly promising as a third-generation solar cell, offering an inexpensive and simple fabrication process. The performance of DSSC has been proven to improve through the optimization of DSSC parts such as photoanode. Therefore, this research aimed to optimize photoanode part of DSSC using random forest method through machine learning predictions. The optimization process was carried out through combinations of single and double layers to identify top-performing configurations. The two top prediction outcomes were A3 with DN-F05 0.8 mM) and double layer configurations combining A3+A2 with DNF-05 0.8 mM. Furthermore, the two combinations were fabricated and characterized using UV-VIS, FT-IR, and I-V test meters. The results of UV-VIS measurement indicated a typical peak of DNF-05 at a wavelength of 482 nm, while FT-IR spectra showed the presence of TiO_2 groups and dyes. Based on the results, the highest power conversion efficiencies of 3.062% were obtained in single layer.

Keywords: Dye-sensitized solar cell; Random forest; DN-F05 dye.

1. Introduction

The global energy demand is growing at an unprecedented rate, driven by rapid economic development and population growth[1-3]. The primary source of energy consumption, fossil fuels, is responsible for the depletion of non-renewable natural resources and an increase in environmental harm[4-5]. Therefore, the world today stands at a critical juncture, facing the dual challenge of meeting the ever-increasing energy demand and mitigating the adverse impacts of climate change[6-8]. This underscores the importance of limiting and reducing the use of fossil fuels and transitioning to abundant, sustainable, and ecologically friendly renewable energy sources[9-11]. Therefore, solar energy has become a major focus in various communities advocating for renewable energy adoption[12].

Solar cell is the leading alternative to using renewable energy, capable of converting sunlight into electric current through the photovoltaic effect. Solar cell technology is a cornerstone of the global effort to transition towards cleaner and more sustainable energy systems[13-14]. The amount of energy produced from sunlight is significant, making solar cells an alternative source for the future. Additionally, the use of solar cells contributes to preventing global warming due to environmentally friendly nature[15].

The different varieties of solar cells available include first, second, and third generation. Among these varieties, dye-sensitized solar cells (DSSC) have shown significant potential compared to others[16]. The benefits of DSSC include low cost and easy manufacture, abundance of material, transparency, high photo-conversion efficiency, low toxicity, as well as the ability to operate in diffuse and artificial light[17-22].

DSSC component that plays the most important role in the generation and charge transfer process is photoanode[23]. Therefore, research has focused on optimizing the photoanode to increase the power conversion efficiency of DSSC. TiO_2 has become a

preferred semiconductor layer for the DSSC working electrode due to its low cost, high photocatalytic activity, thermal, and chemical stability[24]. Another component is dye, which is sensitive to light and initiates electron excitation mechanisms after photons are absorbed. Previous research has shown that the use of Dyenamo dye (DN-F05) with various concentrations provides excellent performance due to the significant effect on optical properties[25].

Several investigations have been carried out to improve the performance of photoanode, focusing on optimizing the materials used. Machine learning for photoanode optimization has not received much attention in research. The application of machine learning can enhance resource efficiency by identifying the optimal parameters for DSSC performance, thereby reducing the necessity for extensive trial and error[26-27]. Using decision trees and support vector training methods such as Maddah research (2022), which leverages machine learning investigation to optimize the possibility of much higher PCE[28]. According to Li et al. (2019), the utilization of Machine Learning techniques in the design and fabrication of solar cells has proven to be highly effective[29]. Besides minimizing costs and time, the application of Machine Learning techniques accuracy due to the ability of random forests method to combine predictions from several decision trees. This approach reduces the risk of overfitting and increases the model's resilience. Research conducted by Kandregula et al. (2022) demonstrates that the Random Forest method emerged as the optimal technique, providing the most precise predictions for suggesting new DSSC dye molecules with enhanced efficiency[31]. Al-Sabana & Abdellatif (2022), in their study, employed the random forest algorithm to enhance the performance of DSSC concerning conversion efficiency. Optimization was carried out on the thickness and porosity of the mesoporous TiO_2 active layer. The random forest method exhibited an accuracy rate of 99.87%, in good agreement with the observed experimental data[32].

In general, experimental research is carried out by varying the conditions of DSSC samples. This process is often time-consuming, labor-intensive, and expensive[29]. However, by using machine learning approaches like Random Forests, researchers can efficiently explore and identify optimal parameter combinations without repeatedly conducting experiments. Random Forest methods have the advantage of dealing such complexity by distinguishing intricate patterns and interactions between variables, which may be difficult or even impossible to detect through traditional experimental methods. In addition, using machine learning approach allows researchers to save resources such as time, finances, and materials that are usually used in experiments. While experimental research remains important in validating results and comprehending the physical mechanisms underlying DSSC efficiency, research utilizing machine learning methods such as random forests assume its own

significance in expediting the optimization process, conserving resources, and providing deeper insights into these systems.

Therefore, this research aimed to optimize photoanode through the use of machine learning predictions and the random forest method. The learning feature data uses two models, namely TiO_2 layer variation and dye concentration DN-F05. These models are used to predict open circuit voltage (Voc) and short circuit current density (Jsc) from several variations.

2. Methodology

2.1 Materials

The materials used included fluorine-doped tin oxide (FTO) was purchased from Greatcellsolar Materials, with dimensions of L(length) 100 mm x W(width) 100 mm x T(thickness) 2.2 mm and sheet resistance of 7 Ω/square. The two types of transparent titania paste used were TiO_2 T/SP (Solaronix) and TiO_2 18NR-T (greatcellsolar materials). Additionally, two types of reflector titania paste used were TiO_2 R/SP (Solaronix) and TiO_2 WER2-O (greatcellsolar materials). Platinum (DN-CE01) and organic dye (DN-F05) were obtained from Dyenamo. Electrolyte and sealing films were Mosalyte TDE-250 and Meltonix 1170-60, respectively, purchased from Solaronix. Other chemicals used included 70% ethanol (merck), tert-buthanol (merck), and acetonitrile (fulltime).

2.2 Fabrication of DSSC

The FTO-coated glass substrate 30 x 2.5 x 2.2 mm, was sonicated after being submerged in 70% ethanol for 30 minutes. The working electrode layer was marked with scotch tape to form an area of (0.7x0.7) cm^2. The doctor blade method was used for the deposition of TiO_2 paste onto conductive glass. The variation of TiO_2 layer used was coded as shown in Table 1. Meanwhile, platinum paste was used after drilling and coating the FTO glass for counter electrode. The FTO-coated glass with TiO_2 and Platinum was heated in a furnace at a temperature of 450°C for 45 minutes. The dye layer was prepared by dissolving DN-F05 of 3 mg (0.5 mM), 4 mg (0.8mM), 6 mg (1mM), and 7 mg (1.2mM) into the solvent tert-buthanol and acetonitrile (1:1) of 5 ml and stirred for 2 hours at a temperature of 40°C. Soaking in a dye solution was carried out for 24 hours, followed by substrate cleaning using ethanol. The working electrode substrate and counter electrode were stacked with the addition of a spacer between the two layers using a sealing film (spacer). These sandwich configurations were hot pressed to melt sealing film to protect both layers from short circuits and leakage of electrolyte. Subsequently, electrolyte was injected through drilled holes closed with cover glass. The complete fabrication of DSSC cells is shown in Fig.1.
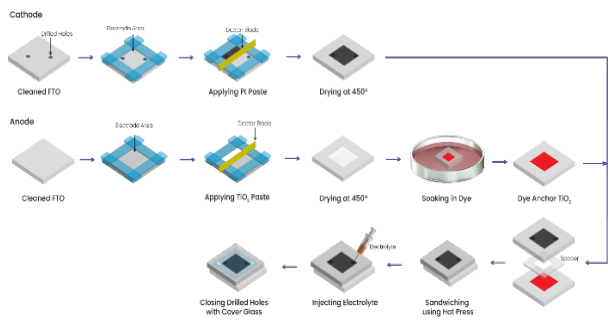
Fig 1: DSSC fabrication process

Table 1. TiO$_2$ sample code

Sample	Code
TiO$_2$ T/SP	A1
TiO$_2$ R/SP	A2
TiO$_2$ 18NR-T	A3
TiO$_2$ WER2-O	A4

2.3 Optimization Model

The working electrode used comprised six variations of TiO$_2$ layer, as shown in Table 1. The dye used for each variation of TiO$_2$ was of different concentrations, ensuring no identical DSSC cells among the 19 samples. Performance testing of 19 DSSC cells was carried out under 35 Watt Xenon lamp irradiation, followed by measurement of Voc and Isc using a multimeter. The value of Isc was divided by the active area which resulted in the value of Jsc. These values of Voc and Jsc were used as input for the optimization model process.

In this research, Python application was used to carry out the processing model stage using the random forest method. A process flow diagram of the Random Forest method is presented in Fig. 2. The random forest method is a machine learning technique grounded in ensemble learning, employing numerous decision trees to generate predictions. The initial steps in utilizing the random forest method involve Feature Selection, which requires identifying and extracting related features from the dataset. In this study, the dataset consists of variations in the TiO$_2$ layer and the DN-F05 dye concentration. Subsequently, the selected dataset is partitioned into two subsets: one for training purposes and the other for testing or validation. The majority of the data is allocated for model training, while a smaller portion is reserved for evaluating the resulting model's performance.
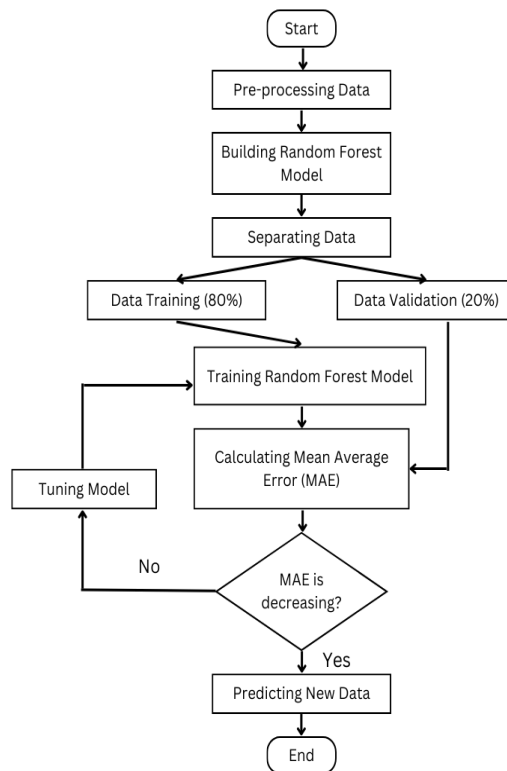

Fig 2: Processing model flow chart with random forest method

Following data partitioning, the subsequent step involves constructing a random forest model. This model consists of several decision trees derived from subsets of the training data. Each decision tree is trained on a random sample of the training dataset, with features selected randomly during each iteration. This approach helps reduce overfitting and enhancing model generalization. Each decision tree is trained on a subset of the training data using distinct learning algorithms. This iterative process involves segmenting the data into smaller subsets based on randomly selected criteria and identifying features that produce optimal differentiation between dataset classes.

Once all decision trees are trained, the predictions from each tree are combined to produce a final prediction. For regression tasks such as DSSC efficiency prediction, the predictions from each tree are averaged. Subsequently, the constructed model undergoes evaluation using a previously designated subset of testing data. This evaluation can be conducted using various performance metrics, such as mean absolute error (MAE) used in this study.

Therefore, the random forest method can be used for DSSC optimization using complex datasets, distinguishing complex patterns, and providing accurate predictions regarding solar cell efficiency based on specified conditions and parameters.

The process of predicting the value produced by the random forest method using the two best optimization

models is known as the post-processing model. Subsequently, the optimal optimization model is recreated and put to the test using FT-IR spectra measurements, UV-vis absorption measurement (Shimadzu UV-1800), and I-V characterization under a 1000 watt/m^2 Xenon light (Keithley 2602A).

3. Result and Discussion

The results of the optimization model and analysis of the research conducted were presented in this chapter.

3.1 Performance of DSSC with TiO$_2$ Layer Variation

Based on the values of Voc and Jsc, the performance of 19 samples was assessed. TiO2 layer variation and dye concentration fluctuation constituted the two sections of the evaluation. This provided two learning features for the constructed model to facilitate the optimization process.

The first variation used as a learning feature was the TiO$_2$ layer variation. In this research, five variations of TiO$_2$ layer (A1; A1+A2; A2+A3; A3; A3+A4) were used as the working electrode. Each variation was evaluated for performance based on the resulting Voc and Jsc. The results of the evaluation of TiO$_2$ layer variations on the Voc value are presented as follows:
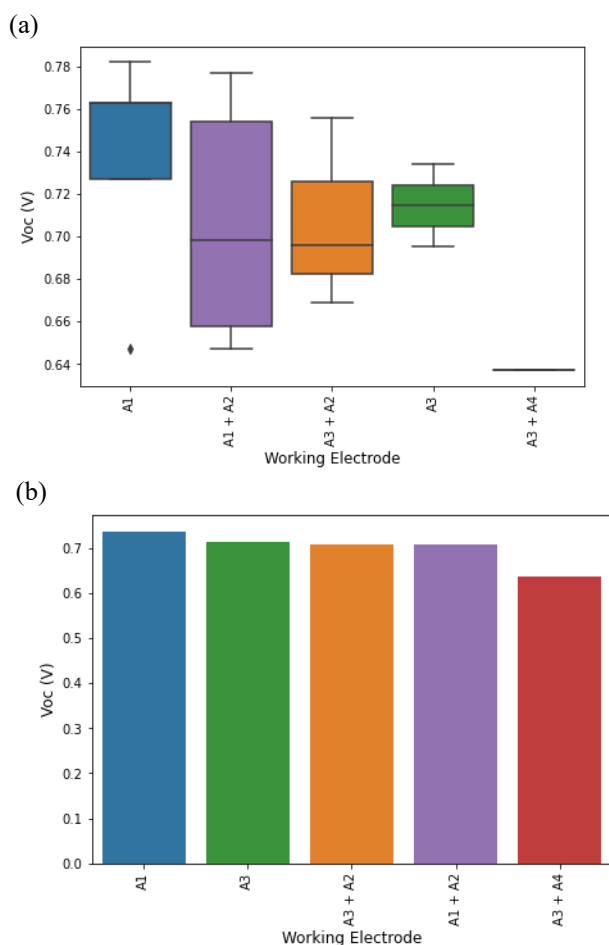
(a)

(b)

Fig 3: Evaluation graph of Voc (a) median value (b) mean value with TiO$_2$ layer variation

Figure 3 showed that A1 variation occurred where the median value of Voc was the largest, indicating the highest average value. These results showed that the use of TiO$_2$ layer A1 provided the maximum Voc value compared to other variations. The excited electrons from the dye moved to TiO$_2$ through a diffusion process. In this case, the porosity of TiO$_2$ semiconductor layer played an important role in the resulting Voc. Furthermore, the size and quantity of particles in TiO$_2$ determined its porosity level, influencing the thickness of the semiconductor layer and the Voc value. Therefore, a significant decrease is observed in Voc due to the increased length of electron transport path caused by high TiO$_2$ thickness. This phenomenon is influenced by the size and number of particles, facilitating easier electron recombination with the electrolyte[33]. The results of the evaluation of TiO$_2$ variations on the resulting Jsc value are presented as follows:
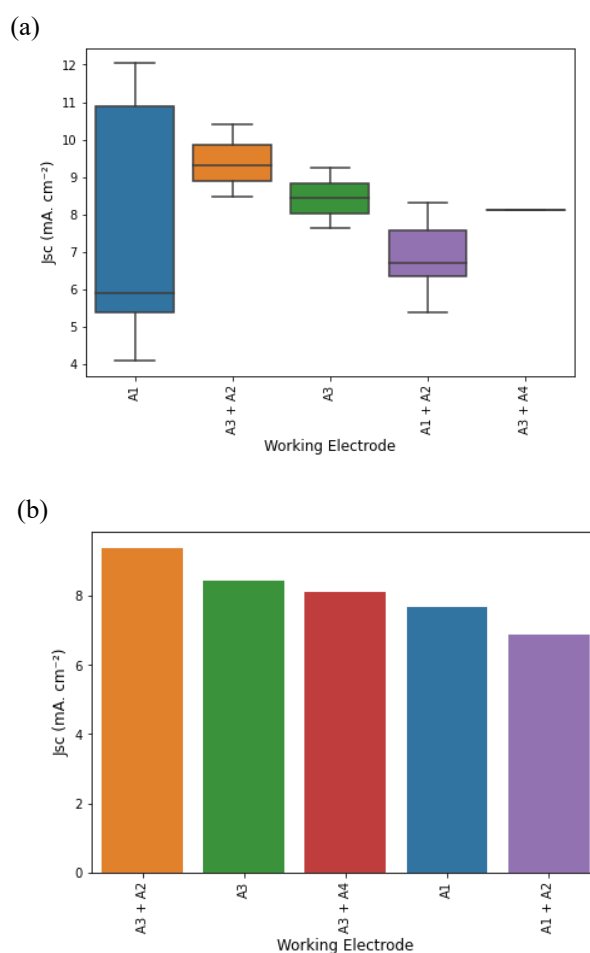
(a)

(b)

Fig 4: Evaluation graph of Jsc (a) median value (b) mean value with TiO$_2$ layer variation

Figure 4 shows that the working electrode A1 variation shows the largest median value of Jsc. However, the highest average value of Jsc is produced on the variation A3+A2. The use of working electrode A3+A2 is more stable to obtain Jsc results compared to others. Meanwhile, the average result of Jsc on the use of the A1 working

electrode is in the fourth position. In practice, a higher value of Voc has a relatively smaller Jsc due to the potential to limit the conversion efficiency[29]. The value of Jsc can also increase with high TiO_2 thickness. This is because thicker working electrode absorbs more excitation electrons from the dye, resulting in a higher Jsc value.

3.2. Performance of DSSC with Dye Concentration Variation

The second variation used as a learning feature is Dyenamo dye concentration (DN-F05). In this research, 4 variations of dye concentration were used, namely 0.5 mM, 0.8 mM, 1 mM, 1.2 mM. Each variation was evaluated for performance based on the resulting Voc and Jsc values. The results of the variation of dye concentration on the resulting Voc value are shown as follows:
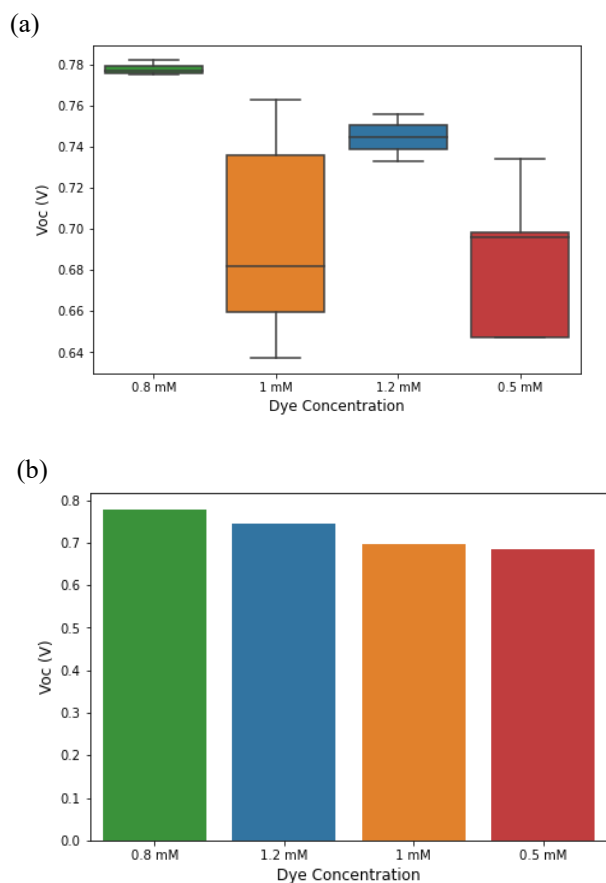
(a)

(b)

Fig 5: Evaluation graph of Voc (a) median value (b) mean value with dye concentration variation

Figure 5 shows that the median value of the highest Voc at the dye concentration variation is 0.8 mM. The highest average Voc value was produced at a variation of 0.8 mM dye concentration. Meanwhile, the evaluation results of variations in dye concentration on the value of Jsc are as follows:
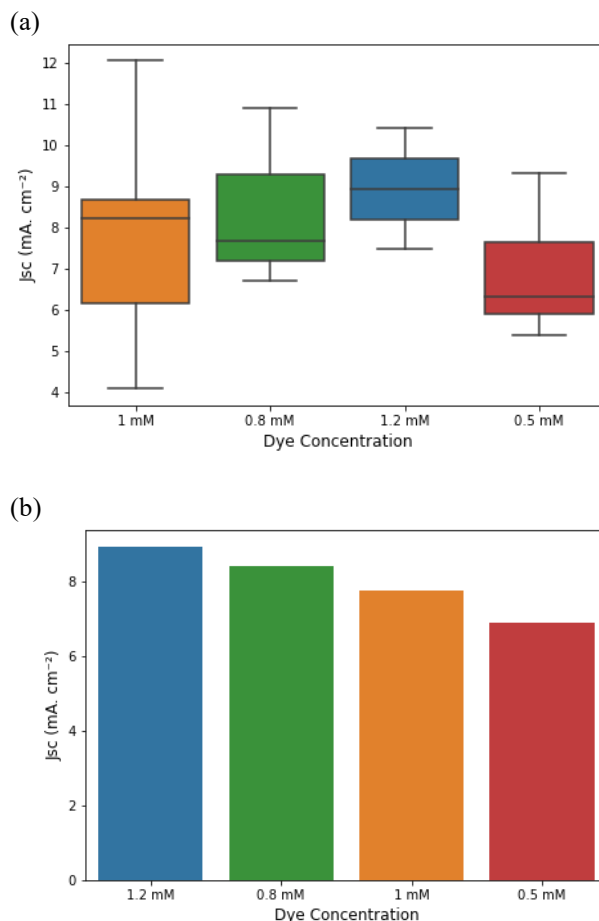
(a)

(b)

Fig 6: Evaluation graph of Jsc (a) median value (b) mean value with dye concentration variation

As shown in Figure 6, the median value of Jsc is highest at the 1 mM dye concentration variation. The highest average value of Jsc was produced at a variation of 1.2 mM dye concentration. This showed that the use of variations in dye concentration of 0.8 mM was more effective, indicating relatively stable Jsc. The stability is attributed to a low electron mobility value, resulting in a higher Voc. Additionally, the scattering effect at a dye concentration of 0.8 mM is more effective, influencing the penetration of light into the scattering layer[34].

3.3 Model Optimization

Model optimization was carried out based on the performance analysis of 19 samples. In optimizing the model, two learning features were used, namely TiO_2 layer and dye concentration variations. Voc and Jsc, the performance results produced by these two characteristics, were used as training data and model validation. Prediction values were run on 25 potential combinations after obtaining the model and the results obtained for the five highest scores are as follows:

Table 2. The five highest prediction values for each variation combination

Working Electrode	Dye Concentration (mM)	Voc Prediction (V)	Jsc Prediction (mA. cm^{-2})
A3 + A2	0.8	0.7731	9.7126
A3	0.8	0.7750	9.1312
A3+A5	0.8	0.7723	9.1005
A1	0.8	0.7763	9.0448
A3+A2	1.2	0.7186	9.1159

The prediction results using the random forest method showed that combination with the highest performance results, namely variation of TiO_2 A3+A2 with a dye concentration of 0.8 mM. This was followed by the selection of the two most probable pairings derived from the estimated value. The two combinations fall outside of 19 samples that were used to obtain learning data. Therefore, these combinations were fabricated according to the previously performed procedure namely single layer (A3 with DNF-05 0.8 mM) and double layer (A3+A2 with DNF-05 0.8 mM). The two combinations fabricated were tested for characteristics using the UV-Vis, FT-IR measurement, and the I-V meter test.

3.4 Absorbance Characterization

The absorption spectra of DN-F05 loaded TiO_2 18NR-T are shown in Fig. 7, determined in the 200–800 nm wavelength range using a Shimadzu UV–1800 UV-Vis spectrophotometer.
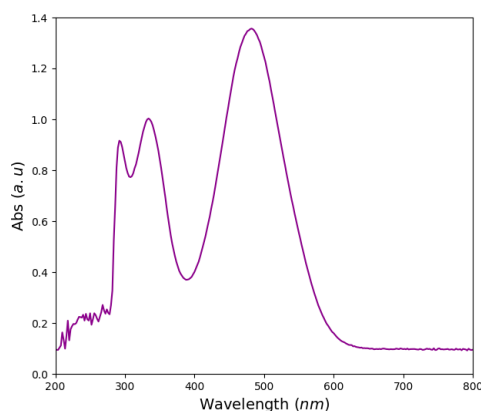

Fig 7: Optical absorption spectra of single layer of A3 with DNF-05 0.8 mM

The absorption spectra obtained have a peak intensity of 482 nm, a typical characteristic of DN-F05[35], indicating that DN-F05 is anchored to the TiO_2 layer. Furthermore, the broad peak in the range of 400-550 nm shows that DN-F05 absorbs light in the visible region[36].

3.5 I-V Characterization

The typical photocurrent density-photovoltage curves for the produced DSSCs are shown in Fig. 8. Meanwhile, Table 3 summarizes the relevant photovoltaic parameters of two different types of DSSC.
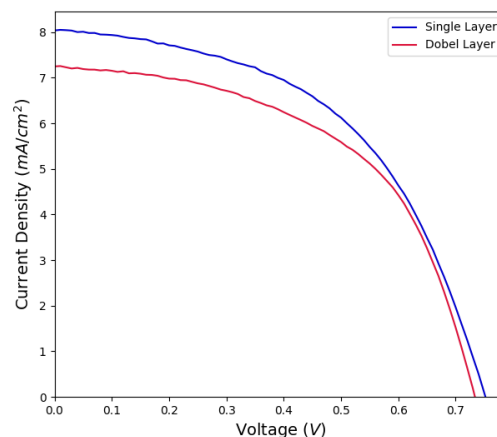

Fig 8: I-V characteristics of single layer and double layer samples

Table 3. DSSC performance of single layer and double layer samples

Sample Code	Jsc (mA/cm^2)	Voc (Volt)	FF (%)	Eff (%)
Single Layer	8.036	0.752	50.67	3.062
Double Layer	7.247	0.733	53.08	2.822

The power conversion efficiencies of DSSC with double layer (TiO_2 18NR-T and TiO_2 R/SP) and single layer (TiO_2 18NR-T) were 2.822% and 3.062%, respectively. The results showed that double layer performance was higher compared to single layer performance. The configuration of double layer of TiO_2 increased the amount of light absorbed in the front transparent layer by TiO_2 R/SP[37]. The large size of TiO_2 R/SP nanoparticles as reflective layer effectively trapped more incident light, thereby exciting more electrons[38].

The high performance of double layer is attributed to the addition of a reflective layer, which increases the thickness of TiO_2 layer and minimizes light transmission. Increasing the thickness of the TiO_2 layer which is not optimal can also lead to higher resistance inhibiting charge transfer. To overcome this limitation, there is a need to control the optimal thickness of TiO_2 layer, as reported by Jeng et al. [39].

According to the prediction, Voc and Jsc values of double layer are 0.7731 V and 9.7126 mA cm^{-2}, respectively. Meanwhile, values of Voc and Jsc of single layer are 0.7750 V and 9.1312 mA cm^{-2}. This discrepancy

is attributed to variations in the method used for measuring light intensity and the distance from the light source. Prediction data for these variables was obtained through manual testing using a multimeter and a 35 Watt Xenon lamp irradiation.

3.6 SEM Characterization

The I-V test results show that single-layer samples perform better than double-layer samples. Therefore, SEM testing was carried out at 1000x and 5000x magnification on single-layer samples. Figure 9 shows the SEM image of a single-layer working electrode sample soaked with 0.8 mM DN-F05. This SEM image characterizes the surface morphology of the sample, which looks dense and slightly porous. It is estimated that the single-layer sample has agglomerated nanoparticles. These nano-sized particles will increase light absorption, and the presence of these pores can increase electron diffusion[38]. Therefore, DSSC performance can be improved.
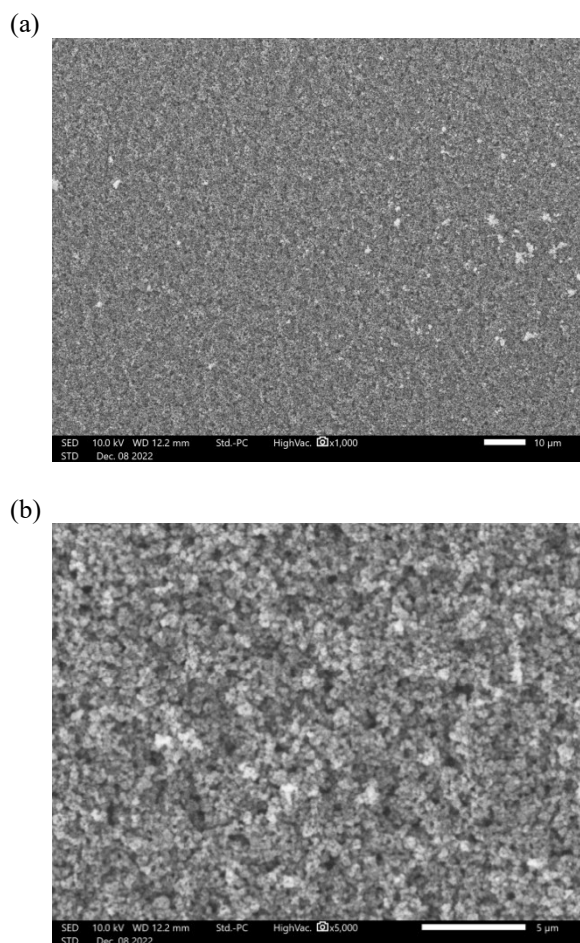
(a)

(b)

Fig 9: SEM images of single layer samples with a magnification of (a) 1000x and (b) 5000x

4. Conclusion

In conclusion, this research used machine learning predictions with the random forest method to optimize the DSSC performance by predicting Voc and Jsc values. The two models, namely the dye concentration DN-F05 variation and the TiO_2 layer proved effective in the optimization process. Based on the prediction result, single layer (A3 with DNF-05 0.8 mM) and double layer (A3+A2 with DNF-05 0.8 mM) were the two combinations with the highest Jsc and Voc values. The results of UV-Vis and FT-IR showed that DNF-05 dye was successfully loaded on the TiO_2 layer. The highest power conversion efficiencies of 3.062% were obtained in single layer. The difference in Voc and Jsc values was attributed to variations in measurement method and DSSC functionality. To minimize error value prediction data and DSSC performance assessment should be carried out using the same measurement method.

References

1) Vo, D. H., & Vo, A. T, "Renewable energy and population growth for sustainable development in the Southeast Asian countries", Energy, Sustainability and Society, **11**(1), 30, 2021, doi : https://doi.org/10.1186/s13705-021-00304-6.

2) Ganivet, E, "Growth in human population and consumption both need to be addressed to reach an ecologically sustainable future", Environment, Development and Sustainability, **22**(6), 4979-4998, 2020, doi : https://doi.org/ 10.1007/s10668-019-00446-w.

3) Arora, N. K., & Mishra, I, "Progress of sustainable development goal 7: clean and green energy for all as the biggest challenge to combat climate crisis", Environmental Sustainability, **5**(4), 395-399, 2022, doi : https://doi.org/10.1007/s42398-022-00257-2.

4) M. Shakeel Ahmad, A. K. Pandey, and N. Abd Rahim, "Advancements in the development of TiO_2 photoanodes and its fabrication methods for dye sensitized solar cell (DSSC) applications. A review," Renew. Sustain. Energy Rev., **77**, 89–108, 2017, doi: 10.1016/j.rser.2017.03.129.

5) G. Dwivedi, G. Munjal, A. Bhaskarwar, and A. Chaudhary, "Dye-sensitized solar cells with polyaniline: A review," Inorg. Chem. Commun., vol. 135, p. 109087, 2022.

6) Fawzy, S., Osman, A. I., Doran, J., & Rooney, D. W, :Strategies for mitigation of climate change: a review:, Environmental Chemistry Letters, **18**, 2069-2094, 2020, doi : https://doi.org/10.1007/s10311-020-01059-w.

7) Zheng, Y., Xu, Q., & Wang, Q, "How is energy transition shaping a path to common prosperity and sustainable economic growth?", Economic Change

and Restructuring, 57(2), **40**, 2024, doi : https://doi.org/10.1007/s10644-024-09624-x.

8) Arora, N. K., & Mishra, I, "Responsible consumption and production: a roadmap to sustainable development", Environmental Sustainability, **6**(1), 1-6, 2023, doi : https://doi.org/10.1007/s42398-023-00266-9.

9) S.K.S. R. Kumar, S. K. Verma, N. K. Gupta, "Performance enhancement of tsah using graphene and graphene / ceo 2 -black paint coating on absorber : a comparative study," Evergreen, **9**(*3*) 673–681, 2022, doi : https://doi.org/10.5109/4843098.

10) Gayen, D., Chatterjee, R., & Roy, S, "A review on environmental impacts of renewable energy for sustainable development", International Journal of Environmental Science and Technology, **21**(5), 5285-5310, 2024, doi : https://doi.org/10.1007/s13762-023-05380-z.

11) Gielen, D., Boshell, F., Saygin, D., Bazilian, M. D., Wagner, N., & Gorini, R, "The role of renewable energy in the global energy transformation", Energy strategy reviews, **24**, 38-50, 2019, doi : https://doi.org/10.1016/j.esr.2019.01.006.

12) K. Marzia, M.F. Hasan, T. Miyazaki, B.B. Saha, and S. Koyama, "Key factors of solar energy progress in bangladesh until 2017," Evergreen, **5**(2) 78–85 (2018). doi:10.5109/1936220.

13) Maka, A. O., & Alabid, J. M, "Solar energy technology and its roles in sustainable development", Clean Energy, **6**(3), 476-483, 2022, doi : https://doi.org/10.1093/ce/zkac023.

14) Nagababu, G., Patil, P., Bhatt, T. N., Srinivas, B. A., & Puppala, H, "Floating solar panels: a sustainable solution to meet energy demands and combat climate change in offshore regions", Journal of Thermal Analysis and Calorimetry, 1-8, 2024, doi : https://doi.org/10.1007/s10973-024-13022-w.

15) T. Hanada, "Modifying the feed-in tariff system in japan: an environmental perspective," Evergreen, **3**(2) 54–58 (2016). doi:10.5109/1800872.

16) Z. Arifin, S. Hadi, Suyitno, B. Sutanto, and D. Widhiyanuriyawan, "Investigation of curcumin and chlorophyll as mixed natural dyes to improve the performance of dye-sensitized solar cells," Evergreen, **9**(*1*) 17–22 (2022). doi:10.5109/4774212.

17) J. Gong, K. Sumathy, Q. Qiao, and Z. Zhou, "Review on dye-sensitized solar cells (DSSCs): Advanced techniques and research trends," Renew. Sustain. Energy Rev., vol. 68, no. October 2016, pp. 234–246, 2017, doi: 10.1016/j.rser.2016.09.097.

18) L. Ju, M. Li, L. Tian, P. Xu, and W. Lu, "Accelerated discovery of high-efficient N-annulated perylene organic sensitizers for solar cells via machine learning and quantum chemistry," Mater. Today Commun., vol. 25, no. September, p. 101604 (2020) doi: 10.1016/j.mtcomm.2020.101604.

19) C. V. Jagtap, V. S. Kadam, S. R. Jadkar, and H. M. Pathan, "Performance of N3 Sensitized Titania Solar Cell under Artificial Light Ambience," ES Energy Environ, 2019, doi: 10.30919/esee8c220.

20) C. Hora, F. Santos, M. G. F. Sales, D. Ivanou, and A. Mendes, "Dye-sensitized solar cells for efficient solar and artificial light conversion," ACS Sustain. Chem. Eng., vol. 7, no. 15, pp. 13464–13470, 2019, doi: 10.1021/acssuschemeng.9b02990.

21) N. Akter, A. Hossion, and N. Amin, "Fabrication of oxide passivated and antireflective thin film coated emitter layer in two steps for the application in photovoltaic," *Evergreen*, 9(3) 654–661 (2022). doi:10.5109/4842524

22) Sharma, K., Sharma, V., & Sharma, S. S, "Dye-sensitized solar cells: fundamentals and current status", Nanoscale research letters, 13, 1-46, 2018, doi : https://doi.org/10.1186/s11671-018-2760-6.

23) W. Ghann et al., "The synthesis and characterization of carbon dots and their application in dye sensitized solar cell," Int. J. Hydrogen Energy, vol. 44, no. 29, pp. 14580–14587, 2019, doi: 10.1016/j.ijhydene.2019.04.072.

24) M. C. Wu, W. C. Chen, T. H. Lin, K. C. Hsiao, K. M. Lee, and C. G. Wu, "Enhanced open-circuit voltage of dye-sensitized solar cells using Bi-doped TiO_2 nanofibers as working electrode and scattering layer," Sol. Energy, vol. 135, pp. 22–28, 2016, doi: 10.1016/j.solener.2016.05.021.

25) D. G. Saputri, A. Supriyanto, M. K. Ahmad, N. E.-H. Diyanahesa, and F. Ramadhani, "Optical properties of dye DN-F05 as a good sensitizer," J. Phys. Theor. Appl., vol. 3, no. 2, p. 43, 2019, doi: 10.20961/jphystheor-appl.v3i2.38145.

26) Zhang, Y., Fu, H., Zhang, M., Yang, Q., & Hu, W, "Deep-learning-assisted photovoltaic performance prediction of sensitizers in dye-sensitized solar cells", New Journal of Chemistry, 2024, doi : https://doi.org/10.1039/D4NJ01518E.

27) Rondán-Gómez, V., Montoya De Los Santos, I., Seuret-Jiménez, D., Ayala-Mató, F., Zamudio-Lara, A., Robles-Bonilla, T., & Courel, M, "Recent advances in dye-sensitized solar cells", Applied Physics A, 125, 1-24, 2019, doi : https://doi.org/10.1007/s00339-019-3116-5.

28) H. A. Maddah, "Machine learning analysis on performance of naturally-sensitized solar cells," Opt. Mater. (Amst)., vol. 128, no. April, p. 112343, 2022, doi: 10.1016/j.optmat.2022.112343.

29) Li, F., Peng, X., Wang, Z., Zhou, Y., Wu, Y., Jiang, M., & Xu, M, "Machine learning (ML)-assisted design and fabrication for solar cells," Energy & Environmental Materials, 2(4), 280-291, 2019, doi: 10.1002/eem2.12049.

30) Sutar, S. S., Patil, S. M., Kadam, S. J., Kamat, R. K., Kim, D. K., & Dongale, T. D, "Analysis and prediction of hydrothermally synthesized ZnO-based dye-sensitized solar cell properties using statistical

and machine-learning techniques, " ACS omega, 6(44), 29982-29992, 2021, doi: 10.1021/acsomega.1c04521.

31) Kandregula, G. R., Murugaiah, D. K., Murugan, N. A., & Ramanujam, K, "Data-driven approach towards identifying dyesensitizer molecules for higher power conversion efficiency in solar cells," New Journal of Chemistry, 46(9), 4395-4405, 2022, doi: 10.1039/D1NJ05498H.

32) Al-Sabana, O., & Abdellatif, S. O, "Optoelectronic devices informatics: optimizing DSSC performance using random-forest machine learning algorithm," Optoelectronics Letters, 18(3), 148-151, 2022, doi: 10.1007/s11801-022-1115-9.

33) M. Belarbi, B. Benyoucef, A. Benyoucef, T. Benouaz, and S. Goumri-Said, "Enhanced electrical model for dye-sensitized solar cell characterization," Sol. Energy, vol. 122, pp. 700–711, 2015.

34) K. J. Hwang, D. W. Park, S. Jin, S. O. Kang, and D. W. Cho, "Influence of dye-concentration on the light-scattering effect in dye-sensitized solar cell," Mater. Chem. Phys., vol. 149, pp. 594–600, 2015, doi: 10.1016/j.matchemphys.2014.11.013.

35) A. V. Leandri, P. Liu, A. Sadollahkhani, L. Kloo, and J. M. Gardner, "Excited State Dynamics of [Ru(bpy)3]2+ Thin Films on Sensitized TiO_2 and ZrO2," Chem. Phys. Phys. Chem.

36) H. Min, M. M. Thein, M. T. Phoo, and T. Z. Oo, "Effect of Chelating Agent on Surface Morphology and Electrochemical Properties of TiO 2 Nanotube Arrays," Yadanabon Univ. Res. J., vol. 10, no. 1, 2019.

37) I. Zama, C. Martelli, and G. Gorni, "Preparation of TiO_2 paste starting from organic colloidal suspension for semi-transparent DSSC photo-anode application," Mater. Sci. Semicond. Process., vol. 61, no. January, pp. 137–144, 2017, doi: 10.1016/j.mssp.2017.01.010.

38) M. N. Mustafa and Y. Sulaiman, "Review on the effect of compact layers and light scattering layers on the enhancement of dye-sensitized solar cells," Sol. Energy, vol. 215, pp. 26–43, 2021.

39) Jeng, Ming-Jer, et al. "Particle size effects of TiO_2 layers on the solar efficiency of dye-sensitized solar cells." International Journal of Photoenergy 2013 (2013) doi: 10.1155/2013/563897.